GSN Gene Frameshift Mutations in Alzheimer's Disease

Yaling Jiang, Meidan Wan, Xuewen Xiao, Zhuojie Lin, Xixi Liu, Yafang Zhou, Xinxin Liao, Jingyi Lin, Hui Zhou, Lu Zhou, Ling Weng, Junling Wang, Jifeng Guo, Hong Jiang, Zhuohua Zhang, Kun Xia, Jiada Li, Beisha Tang, Bin Jiao*, Lu Shen*

Include:

Supplementary methods

Supplementary Figure S1-6

Supplementary Table S1

Supplementary methods

ATN framework diagnosis classficiation

The β amyloid deposition, pathologic tau, and neurodegeneration (ATN) framework[1] was described below: Aβ42 level in CSF < 651 pg/ml, or Aβ42/Aβ40 ratio ≤ 0.1, is defined as positive amyloidosis (corresponding to A+ in the ATN framework); p-tau > 61 pg/ml in CSF is defined as neurofibrillary tangles (corresponding to T+ in the ATN framework); t-tau ≥ 290 pg/ml in CSF is defined as nerve cell death (corresponding to N+ in the ATN framework).

Cognitive Impairment Multicenter Database and Collaborative Network in China (CI-MDCNC)

The CI-MDCNC cohort recruited 884 AD patients from 8 clinical sites across China, which is one of the largest multicenter, observational, longitudinal, and natural history studies of AD in China.

Alzheimer's Disease Sequencing Project (ADSP) public database

The ADSP performed whole exome sequencing (WES) of DNA specimens obtained from 5,778 AD cases and 5,136 controls, including 5,519 AD cases and 4,917

cognitively normal elderly controls of European ancestry (EA) and 218 AD cases and 177 controls of Caribbean Hispanic (CH) heritage[2-4].

Targeted gene sequencing

The targeted gene sequencing panel includes four genes (GSN, APP, PSEN1, and PSEN2). The specific methods were described previously[5]. In brief, the genomic DNA was broken into 200-250 bp length fragments by Covaris LE220 (MA, USA). End-repairing, A-tailing, adaptor ligation, and a 15-cycle pre-capture PCR amplification were performed in fragmented DNA. The products were captured by the targeted gene sequencing panel and sequenced on Illumina HiSeq X Ten Analyzers (Illumina, San Diego, CA, USA) after quality control. Then, the bioinformatics processing and data analysis were performed.

3D model structure

The three-dimensional (3D) models of the mutant protein structures were built by Discovery Studio software. We used homology models of gelsolin in the Protein Data Bank (PDB; No. 3ffn) to construct the 3D structure of the mutant proteins by Discovery Studio software. The known 3D model of the GSN D214N mutant protein was from the PDB (No. 6qbf).

Global cerebral atrophy-frontal sub-scale (GCA-F)

The GCA-F scale is defined in the frontal cortex and sulcal. It ranks 0 to 3, with grade 0 representing no cortical atrophy; grade 1, mild atrophy (dilatation of sulci); grade 2, moderate atrophy (loss of gyri volume); and grade 3, end-stage “knife blade atrophy”.[6, 7]

Posterior atrophy (PA)

The PA scale is defined in the posterior cingulate sulcus, parieto-occipital sulcus, precuneus, and parietal cortex. It ranks atrophy from 0 to 3, with grade 0 showing no cortical atrophy; grade 1, mild parietal cortical atrophy, with mild enlargement of the posterior cingulate and parieto-occipital sulcus; grade 2, substantial parietal atrophy, with substantial enlargement of the posterior cingulate and parieto-occipital sulcus; grade 3, end-stage “knife-blade” atrophy, with extreme enlargement of the posterior cingulate and parieto-occipital sulcus.[8]

Medial temporal lobe atrophy (MTA)

The MTA scale is defined in the hippocampus, parahippocampal gyrus, and surrounding CSF spaces. It ranks the degree of MTA from 0 to 4, with grade 0 denoting no cortical atrophy; grade 1, enlargement of choroid fissure; grade 2, along with enlargement of the temporal horn of the lateral ventricle; grade 3, moderate loss of hippocampal volume; and grade 4, severe loss of hippocampal volume.[9]

Reference:

1. Jack CR, Jr., Bennett DA, Blennow K, Carrillo MC, Dunn B, Haeberlein SB, et al. NIA-AA Research Framework: Toward a biological definition of Alzheimer's disease. Alzheimer's & dementia : the journal of the Alzheimer's Association. 2018;14(4):535-62.

2. Crane P, Foroud T, Montine T, Larson E. Alzheimer's Disease Sequencing Project discovery and replication criteria for cases and controls: Data from a community-based prospective cohort study with autopsy follow-up. Alzheimer's & dementia : the journal of the Alzheimer's Association. 2017;13(12):1410-3.

3. Beecham GW, Bis JC, Martin ER, Choi SH, DeStefano AL, van Duijn CM, et al. The Alzheimer's Disease Sequencing Project: Study design and sample selection. Neurology Genetics. 2017;3(5):e194.

4. Zhang X, Farrell J, Tong T, Hu J, Zhu C, Wang L, et al. Association of mitochondrial variants and haplogroups identified by whole exome sequencing with Alzheimer's disease. Alzheimer's & dementia : the journal of the Alzheimer's Association. 2021.

5. Jiang Y, Jiao B, Liao X, Xiao X, Liu X, Shen L. Analyses Mutations in GSN, CST3, TTR, and ITM2B Genes in Chinese Patients With Alzheimer's Disease. Frontiers in aging neuroscience. 2020;12:581524.

6. Zhu H, Lu H, Wang F, Liu S, Shi Z, Gan J, et al. Characteristics of Cortical Atrophy and White Matter Lesions Between Dementia With Lewy Bodies and Alzheimer's Disease: A Case-Control Study. Frontiers in neurology. 2021;12:779344.

7. Wan MD, Liu H, Liu XX, Zhang WW, Xiao XW, Zhang SZ, et al. Associations of

multiple visual rating scales based on structural magnetic resonance imaging with disease severity and cerebrospinal fluid biomarkers in patients with Alzheimer's disease. Frontiers in aging neuroscience. 2022;14:906519.

8. Koedam EL, Lehmann M, van der Flier WM, Scheltens P, Pijnenburg YA, Fox N, et al. Visual assessment of posterior atrophy development of a MRI rating scale. European radiology. 2011;21(12):2618-25.

9. Scheltens P, Leys D, Barkhof F, Huglo D, Weinstein HC, Vermersch P, et al. Atrophy of medial temporal lobes on MRI in "probable" Alzheimer's disease and normal ageing: diagnostic value and neuropsychological correlates. Journal of neurology, neurosurgery, and psychiatry. 1992;55(10):967-72.

Supplementary Figure S1-6

A

Gene	Primer sequence		Annealing temperature	Size
GSN-K346fs	Forward	5'-AGCTGGCCAAGCTCTACAAG-3'	60 ℃	181 bp
	Reverse	5'-TTCCTCTCCTCCGTGTTTGC-3'		
GSN-P3fs	Forward	5'-ACTTAAGGTCGGCGACCC-3'	56 ℃	454 bp (Mut) 482 bp (WT)
	Reverse	5'-CGTTCAGGTAGTCATCCAGC-3'		
GAPDH	Forward	5'-AGTTAAAAGCAGCCCTGGTGA-3'	60 ℃	131 bp
	Reverse	5'-TCGACAGTCAGCCGCATCT-3'		

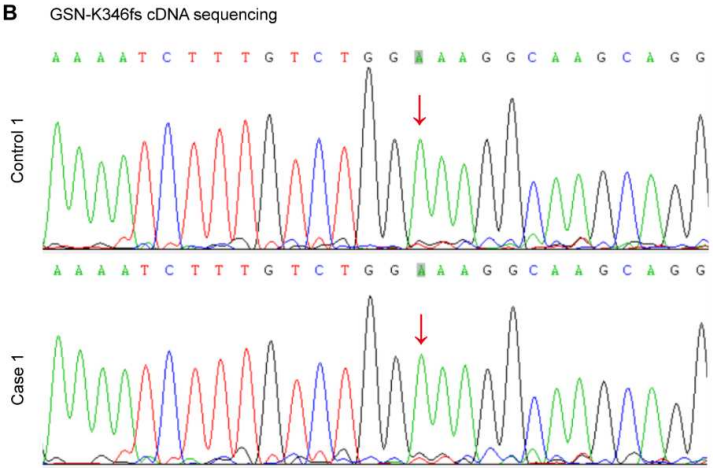

Figure S1 PCR primers and cDNA sequences. **(A)** The PCR primers for GSN frameshift mutations. **(B)** The cDNA sequencing of Case 1 with the K346fs mutation was the same as that of Control 1.

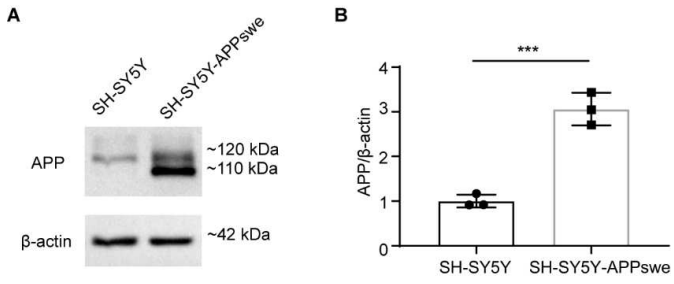

Figure S2 Identification of AD model cells. **(A-B)** Representative western blot (A) and quantification (B) of APP expression in SH-SY5Y and SH-SY5Y-APPswe cells. SH-SY5Y-APPswe cells expressed more APP proteins. *** $P < 0.001$.

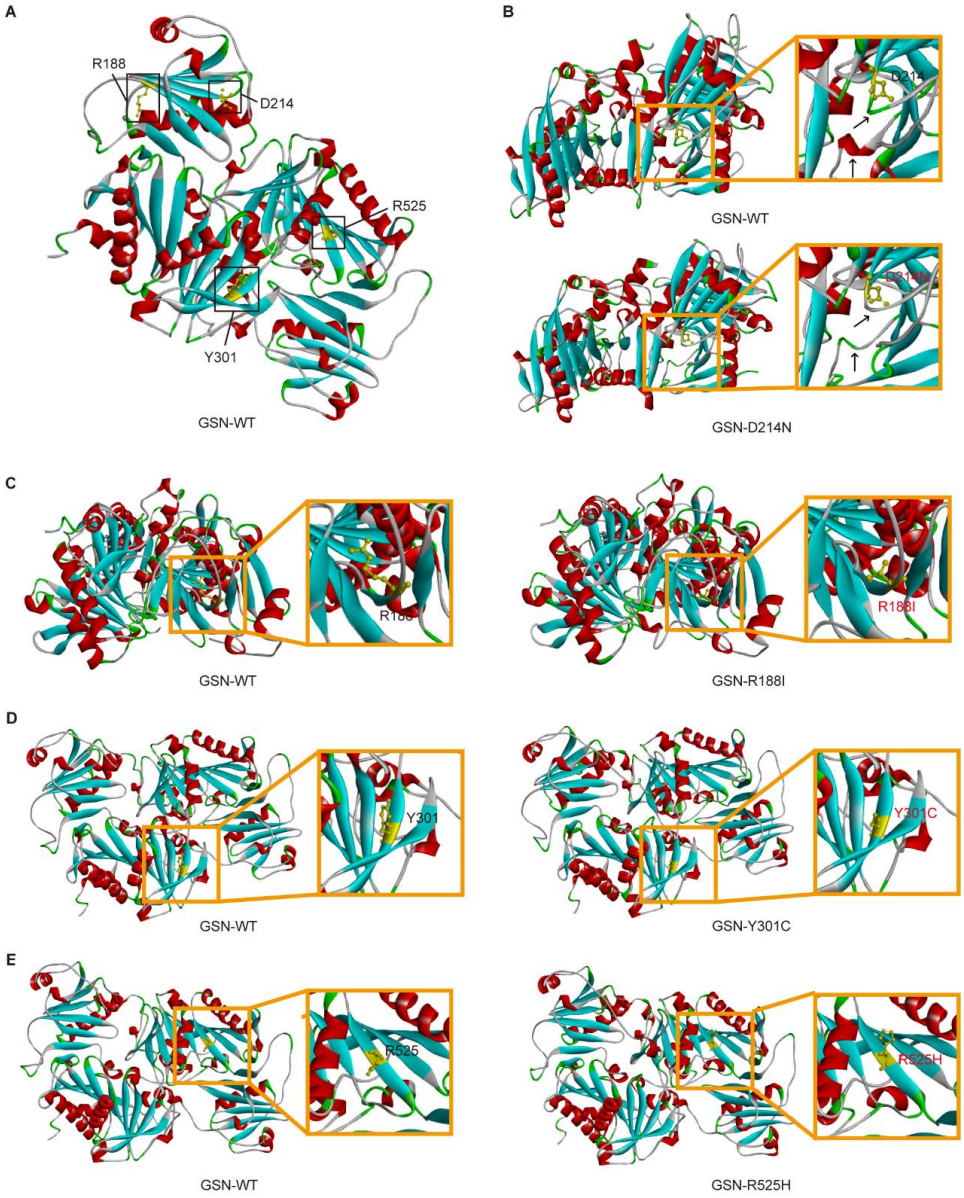

Figure S3 The 3D model of mutant gelsolin proteins. (A) The 3D model of human gelsolin wild type (GSN-WT) from the Protein Data Bank (No. 3ffn). (B) The different 3D configurations between GSN-WT and GSN D214N mutant proteins. The arrows indicate the difference in protein structures between WT and mutant proteins. The different colours of proteins represent different secondary types of proteins. Amino acids of interest are marked in yellow. The orange square indicates the amplification regions. (C-E) Similar 3D configurations between GSN-WT and GSN mutant proteins (D214N (B), R188I (C), Y301C (D), and R525H (E)).

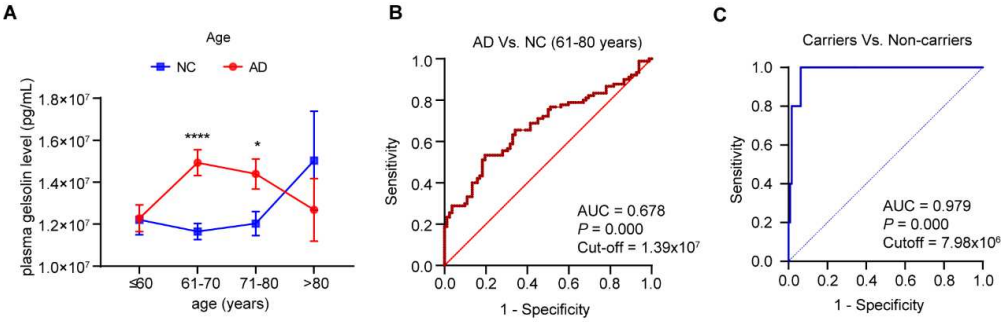

Figure S4 (A) The gelsolin level changes with age in AD patients and NC. The plasma gelsolin level was compensatively increased in the age between 61 to 80 years. In contrast, the gelsolin level was lower than that in the control in the stage more than 80 years. **(B)** The ROC curve of plasma gelsolin levels between AD patients and NC (age 61-80 years) showed a moderate test power to distinguish AD from controls. **(C)** The ROC curve of plasma gelsolin levels between AD patients with *GSN* frameshift mutation carriers and noncarriers showed good test power to distinguish carriers from noncarriers. $^{*}P < 0.05$ versus the NC group, and $^{****}P < 0.001$.

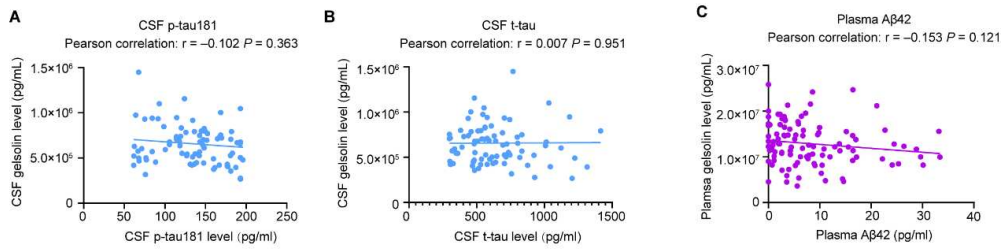

Figure S5 (A) The negative correlation between CSF gelsolin and CSF p-tau181 in AD patients analyzed by Pearson correlation analysis. n = 82. **(B)** The positive correlation between CSF gelsolin and CSF t-tau in AD patients analyzed by Pearson correlation analysis. n = 82. **(C)** The negative correlation between plasma gelsolin and plasma Aβ42 in AD patients analyzed by Pearson correlation analysis. n = 124.

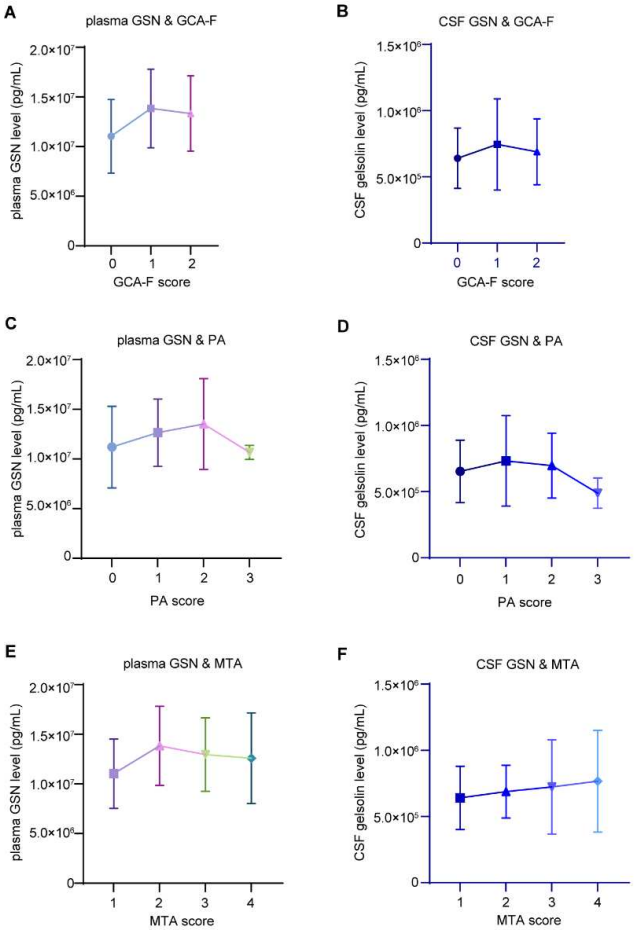

Figure S6 The relationship between gelsolin and brain atrophy. **(A-B)** The gelsolin level (plasma (A) and CSF (B)) changes with GCA-F scores in AD patients. **(C-D)** The gelsolin level (plasma (C) and CSF (D)) changes with PA scores in AD patients. **(E-F)** The gelsolin level (plasma (E) and CSF (F)) changes with MTA scores in AD patients.

Supplementary Table

Table S1 Frameshift mutations of the *GSN* gene in the CI-MDCNC cohort

AA Change	SNP	Mutation type	gnomAD_exome_ALL	gnomAD_exome_EAS	ExAC_ALL	ExAC_EAS	Reve	Functional predictions: pathogenic (total)	Patients	Controls
Frameshift mutations										
exon1:c.8_35del:p.P3fs	rs764841269	Frameshift	0	0	0	0	NA	NA	10	0
exon10:c.1408delG:p.G470fs	rs758669795	Frameshift	4.06E-06	5.79E-05	8.24E-06	1.00E-04	NA	NA	1	0
exon12:c.1655dupC:p.S552fs	rs769989772	Frameshift	1.25E-05	2.00E-04	1.91E-05	3.00E-04	NA	NA	2	0
Carriers (n)									13	0
Frequency (%)									1.47% (13/884)	0.00% (0/1403)
***P* value**									**<0.001*****|	